1972 (Russ. Transl., Mir, M., 1974). A. N. Yutsis and A. A. Bantzaĭtis, Teoriya momenta kolichestva dvizheniya v kvantovoĭ mekhanike (Theory of Angular Momentum in Quantum Mechanics), Vilnyus, 1965.

[18]Yu. Mikhaĭlova and L. Maksimov, Zh. Eksp. Teor. Fiz. 51, 1880 (1966) [Sov. Phys. JETP 24, 1265 (1967)].

Measurements of the ion energy spectrum in a collisionless neutral current sheet

N. A. Koshilev, V. L. Masalov, N. A. Strokin, and A. A. Shishko

Institute of Terrestrial Magnetism, Ionosphere, and Radiowave Propagation, Siberian Division, USSR Academy of Sciences
(Submitted November 23, 1976)
Zh. Eksp.Teor.Fiz. 72, 2110–2119 (June 1977)

A multichannel electrostatic energy analyzer has been used with a θ-pinch installation with a reverse field to determine the ion energy distribution in the radial and longitudinal directions in the plasma. A well-defined beam of ions reflected elastically from the sheet propagates in the radial direction ahead of the neutral sheet. The ion temperature in the sheet does not exceed 60–80 eV. The ion flux along the neutral sheet consists of ions scattered out of the radial flux and ions accelerated across the boundary between the hot and cold plasma.

PACS numbers: 52.25.Lp

Determination of the energy spectra of particles in current sheets with lines of zero magnetic field is a topical problem in connection with attempts to explain some of the phenomena observed in cosmic plasma. They include processes in solar flares and in the tail of the earth's magnetosphere in which, as indicated by existing observational data, neutral current sheets play an important role in particle heating and acceleration. On the other hand, this problem is also connected with the question of turbulent heating of hot plasmas to thermonuclear temperatures at which binary collisions cannot ensure rapid energy dissipation.

It is desirable to elucidate the properties of particle spectra that are characteristic for neutral current sheets, and the physical processes responsible for these properties. Simulation experiments may be helpful in choosing theoretical models of the above phenomena.

Laboratory simulation of processes occurring in neutral current sheets have been described, for example, by Kawashima and Ohyabu,[1] Frank,[2] and Altyntsev and Krasov.[3] The relatively simplest of these experiments is that using the θ-pinch in the configuration of a piston field H_1 and an opposite quasistationary field H_0 frozen into the plasma. In this configuration,[4] measurements of the energy distribution in the electron component of the plasma show that the neutral current sheet is a source of electrons accelerated to energies of about 15 keV. The same configuration has been used to examine the dynamics of the ion components by measuring the Doppler broadening and emission line shift,[5] which indicate the presence of nonthermal particles whose origin is associated with the elastic reflection of a fraction of the ions from the magnetic piston.

In this paper, we report measurements of the energy distribution of the ion component of plasma using the fast charge-transfer atoms leaving the neutral current sheet in longitudinal and transverse directions.

APPARATUS AND DIAGNOSTICS

The experiments were carried out on the θ-pinch installation UN-Phoenix,[6] a diagram of which is shown in Fig. 1. Hydrogen plasma with concentration $n_0 = 2 \times 10^{12} - 2 \times 10^{13}$ cm^{-3} and frozen-in quasistationary field $-H_0 = 150-600$ Oe was produced in the cylindrical glass chamber 1 (diameter 16 cm, length 100 cm). The plasma was compressed by the growing magnetic piston whose field H_1 was opposite in direction to H_0 ($H_1 \uparrow\downarrow H_0$) and was produced by discharging a low-inductance capacitor through the shock coil 4 (length 30 cm) surrounding the central part of the vacuum chamber. The amplitude of the magnetic field of the piston was typically 1200 Oe and the rise time was $T/4 = 400$ nsec. For $|H_1| > |H_0|$ after the piston was switched on, a cylindrical current sheet with a zero field line separating the regions of oppositely directed magnetic fields was produced in the plasma and traveled in the radial direction toward the chamber axis. Depending on the initial density n_0 of the plasma and the quasistationary field H_0, a rarefaction or compression wave propagated ahead of the neutral sheet.

The main parameters of the current sheet in the plasma (width Δ, velocity U, amplitude of magnetic field discontinuity ΔH) were measured with two magnetic probes with an open loop, 3 mm in diameter. The probes were placed successively along the radius of the system at distances $r_1 = 30$ mm and $r_2 = 42$ mm from the axis. The operational control of the initial plasma density n_0 during the measurement process was achieved with the aid of a microwave interferometer ($\lambda = 4$ mm).

The initial electron temperature T_e^0, estimated from microwave absorption in plasma,[7] was 0.5–1.0 eV. The ion temperature T_i^0 was not measured directly, but it was expected that $T_i^0 = T_e^0$ since the lifetime of the plasma (approximately 50 μsec) prior to the introduction of the piston was greater than the temperature relaxation time.

0038-5646/77/4506-1108$02.40
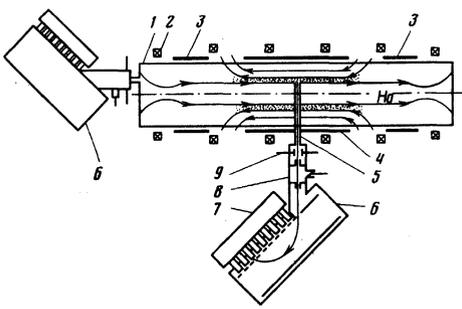
FIG. 1. Diagram of apparatus and diagnostic equipment: 1) vacuum chamber; 2) coils producing quasistationary magnetic field; 3) preionization coils; 4) shock coil; 5) ceramic tube; 6) multichannel energy analyzer for neutral charge-transfer particles; 7) ion detection system; 8) stripping chamber; 9) deflecting capacitor.

The ion energy spectrum was determined from the energy distribution of neutral charge-transfer particles[8] emitted by the plasma. The measurements were carried out with the aid of a multichannel neutral-atom energy analyzer consisting of a stripping chamber 8 and a nine-channel electrostatic ion energy analyzer 6 (Fig. 1) in the form of a plane-parallel capacitor with particle-entrance angle in the analyzing field $\alpha = 45°$.[9] The use of the multichannel instrument ensured that the final results were free from the influence of instabilities in the operation of the system.

The spectrum of ions emitted by the neutral sheet in the radial direction (the "transverse spectrum" $dn_i / d\mathscr{E}_\perp$) was measured by attaching the analyzer to the vacuum chamber in the central section of the shock coil. The neutral charge-transfer particles were extracted through a ceramic tube with an internal diameter of 5 mm, mounted along the radius of the chamber and taken to a distance of $r = 30$ mm in order to exclude cumulative effects. The spectrum of ions emitted along the layer ("longitudinal" spectrum $dn/d\mathscr{E}_\parallel$) was measured in another series of experiments, using the same analyzer placed along the axis of the chamber. The aperture of the instrument was sufficient to enable us to record particles emitted along the entire length of the shock coil from a region of 4×10 mm at a distance $r = 30$ mm from the axis.

It is important to note that the analyzer used in these measurements had a low time resolution ($\Delta t \approx 300$ nsec) because of the long particle flight path and the finite energy resolution of the channels. The resulting ion-energy distribution is, therefore, an average over the entire time interval during which the current sheet moves between the wall of the vacuum chamber and the entrance to the tube. Most of the experimental data were obtained for the average distribution function. The method used to analyze such data under similar experimental conditions is described by Alinovskiĭ et al.[10,11]

A small multichannel analyzer with a high time resolution ($\Delta t \leqslant 30$ nsec) was specially developed[12] and used to examine the spectrum of ions moving in the radial direction in which the particle flight path could be reduced

to a minimum (of the order of the radius of the vacuum chamber). This enabled us to observe the temporal evolution of the transverse spectrum.

EXPERIMENTAL RESULTS

Figure 2 shows typical oscillograms obtained with the magnetic probes. The neutral current sheet formed under these conditions is characterized by widths $\Delta \approx 10 c/\omega_{pe}$ [$\omega_{pe} = (4\pi n e^2/m)^{1/2}$ is the Langmuir frequency of the electrons and c is the velocity of light] and propagation velocity U. The sheet is collisionless.[3] At low initial plasma concentrations ($n_0 < 10^{13}$ cm^{-3}), the neutral sheet is preceded by a rarefaction wave (Fig. 2a). The rarefaction pulse penetrates the plasma with velocity exceeding the Alfven value. This velocity is determined by turbulent processes on the leading front.[13] For $n_0 > 10^{13}$ cm^{-3} ($H_0 = -400$ Oe), the rarefaction wave appears only in the narrow region of the plasma column immediately next to the wall, and when the amplitude $|H_1|$ of the growing magnetic piston begins to exceed $|H_0|$, the perturbation ahead of the neutral sheet is transformed into a collisionless compressional shock wave[14] (Fig. 2b).

The characteristic feature of these experiments is, therefore, the presence of a turbulent zone ahead of the moving neutral sheet, which appears as a result of microinstabilities excited by currents flowing in the rarefaction or compression wave front.

Let us now consider the experimental spectra of ions emitted by the neutral sheet in the radial direction. Figure 3 shows the energy distribution $dn_i/d\mathscr{E}_\perp$ measured for different values of n_0 and typical for this range of magnetic field H_0. The spectra are characterized by a rapid initial fall in $dn_i/d\mathscr{E}_\perp$ and a cutoff $\mathscr{E}_\perp$ at the high-energy end. This suggests that the neutral sheet contains ions accelerated in the direction of its motion. Simultaneous measurements performed with the magnetic probes showed that the energy $\mathscr{E}_\perp$ at which the plateau cuts off is given by $\mathscr{E}_\perp \approx 2MU^2$, where U is the velocity of the sheet. As the initial concentration n_0 (H_0 = const) is increased, the velocity of the current sheet is found to fall and, as is clear from the figure, there is an accompanying reduction in the cutoff energy $\mathscr{E}_\perp$. This behavior may be connected with the elastic reflection of a fraction of the ions from the moving neutral sheet.
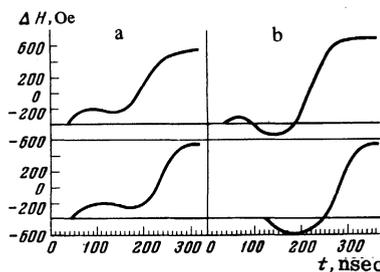
FIG. 2. Typical oscillograms of signals from magnetic probes located at points r_1 (upper curves) and r_2 (lower curves): (a) $n_0 \approx 2 \times 10^{12}$ cm^{-3}, $H_0 = -400$ Oe; (b) $n_0 \approx 2 \times 10^{13}$ cm^{-3}, $H_0 = -400$ Oe.

Koshilev et al.   1109
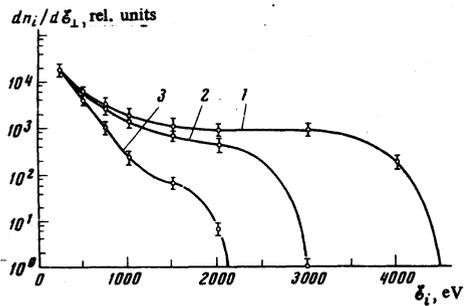
FIG. 3. Energy distributions of ions (normalized to $\mathscr{E} = 260$ eV), $H_0 = -600$ Oe; curve (1) $n_0 \approx 2 \times 10^{12}$ cm^{-3}; curve (2) $n_0 \approx 7 \times 10^{12}$ cm^{-3}; curve (3) $n_0 \approx 2 \times 10^{13}$ cm^{-3}.

This possibility was verified with the aid of the analyzer with high time resolution. The energy spectra corresponding to different times after the introduction of the magnetic piston, and obtained with this instrument in a single operational cycle of the installation, are shown in Fig. 4. At time $t_1 = 120$ nsec after the beginning of the process, there is a well-defined beam of ions with energy $\mathscr{E}_1 \approx 2MU^2$ (curve 1). The elastically reflected ions have laboratory velocities $V = 2U$ and should travel ahead of the current sheet. Magnetic probe data do, in fact, show that the neutral sheet is located in front of the entrance to the ceramic tube at this time. At subsequent times, $t_2 = 220$ nsec (curve 2) and $t_3 = 280$ nsec (curve 3), the ion energy spectrum shifts toward lower energies $\mathscr{E} < 2MU^2$. These distributions characterize the state of the ion component of the plasma after the neutral sheet has traversed the entire region of detection.

To enable us to compare experimental data obtained with different instruments, Fig. 4 gives the distribution averaged over the time interval corresponding to the duration of the recorded signals (curve 4). This is used as an additional check on the validity of the interpretation of the experimental results. On the other hand, comparison shows that analysis of the average spectra cannot be used to establish the presence in plasma of an isolated beam of reflected ions, but the main features of the process can be deduced from these spectra. In particular, the slope of the average spectrum in the cutoff region yields the temperature $T_{\parallel 1}$ of ions in the reflected beam. When the directed velocity of the beam is taken into account, the temperature $T_{\parallel 1}$, determined from the data recorded by both analyzers, is found to lie between 10 and 15 eV.

The temperature $T_{\perp 2}$ of ions in the main mass of plasma dragged by the current sheet can be estimated from the slope of the $dn_i/d\mathscr{E}_\perp$ curves corresponding to the "prompt" spectra (Fig. 4, curve 3). Estimates show that, typically, $T_{\perp 2} \approx 60-80$ eV. It is important to note that the broadening of the spectrum due to heating produces an additional spreading associated with ion charge transfers at different points in the potential discontinuity in the neutral sheet,[5] and also broadening connected with the distortion of the ion distribution function across this discontinuity.[15] These distortions cannot be taken into account because there are no data on the potential

distribution $\varphi = f(r)$ in the sheet and its maximum amplitude φ_m, so that the final value of $T_{\perp 2}$ may be too high.

The relative number of reflected ions n_1/n_2 (n_1, n_2 are the concentrations of particles in the beam and the layer, respectively) can be determined from the "prompt" spectra (Fig. 4) by measuring the ratio of areas under the curves corresponding to the beam (curve 1) and the plasma dragged by the sheet (curve 3). Since the number of particles recorded by the analyzer and having a thermal spread depends on their overall directed velocity,[11] this ratio of areas was determined after the distributions (curves 1 and 3) were transformed to moving coordinate frames attached, respectively, to the reflected beam and the plasma dragged by the sheet. Assuming that the degree of isotropy of the two distributions is the same, calculations show that the ratio n_1/n_2 lies between 0.1 and 0.15.

It is thus possible to extract the main experimental facts from measurements of the transverse spectrum $dn_i/d\mathscr{E}_\perp$. The motion of the neutral sheet is accompanied by elastic reflection and the formation of a separate beam of particles in the plasma in front of the layer. These particles are ions accelerated to energy $\mathscr{E} \approx 2MU^2$. Their density is approximately $0.1n_2 - 0.15n_2$, and their thermal spread is $T_{\parallel 1} \sim 10 - 15$ eV. The main mass of ions is heated in the sheet to $T_{\perp 2} \approx 60-80$ eV.

Let us now consider the longitudinal spectra $dn_i/d\mathscr{E}_\parallel$. When particles emitted along the neutral sheet are recorded, it is found that signals from the analyzer detectors corresponding to the emission of ions from the disturbed plasma have the characteristic double structure shown in Fig. 5. Analysis of the space-time picture of the process has shown that the complex structure of the signals is connected with the simultaneous emission of ions from regions separated by about 15 cm along the line of detection. The first and second peaks on the signals are separated in time on oscillograms from all analyzer channels and are identified with emission from the edge region nearest to the instrument and the central region of the shock coil. This interpretation was confirmed by special measurements of the signal structure as a function of the coil size. When the length of the coil was reduced, the time inter-
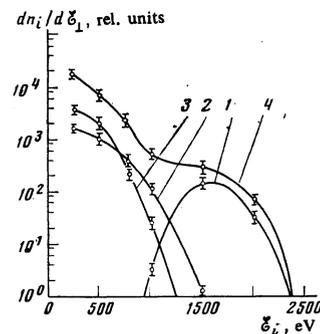
FIG. 4. Temporal evolution of the energy distribution of ions ($H_0 = -150$ Oe, $n_0 = 7 \times 10^{12}$ cm^{-3}): curve (1) $t_1 = 120$ nsec; curve (2) $t_2 = 220$ nsec; curve (3) $t_3 = 280$ nsec.
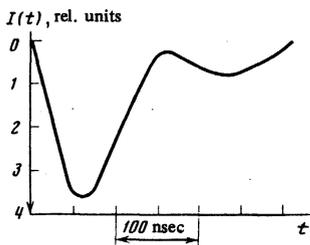
FIG. 5. Oscillogram of the output current $I(t)$ from the detector of the analyzer for a longitudinal flux of ions with $\mathscr{E}_{\parallel}$ =2500 eV.

FIG. 7. Energy distribution of ions (normalized at $\mathscr{E}=260$ eV), $H_0=-600$ Oe; curve (1) $n_0 \approx 2 \times 10^{12}$ cm^{-3}; curve (2) $n_0 \approx 5 \times 10^{12}$ cm^{-3}; curve (3) $n_0 \approx 10^{13}$ cm^{-3}.

val between the peaks was also found to be reduced. The time separation between the peaks could, therefore, be used to determine the two distribution functions corresponding to plasmas emitted by the two regions in a given operational cycle of the system.

Figure 6 shows the energy spectra $(dn_i/d\mathscr{E}_{\parallel})_2$ determined from the second peak on the oscillograms (central region of the short coil). These curves were obtained for constant H_0 and different values of plasma concentration n_0. The first point to note is that the longitudinal and transverse spectra, $(dn_i/d\mathscr{E}_{\parallel})_2$ and $dn_i/d\mathscr{E}_{\perp}$, have identical properties: they have similar shapes for similar values of n_0 and H_0 (Figs. 3 and 6, curve 1). The energy at which the plateau cuts off on longitudinal spectrum is given by $\mathscr{E}_{\parallel} \approx 2MU^2$, where U is the velocity of the neutral sheet. Further examination reveals that the relative intensity of the longitudinal ion flux, estimated with allowance for the volume of the emitting plasma, is higher by two orders of magnitude than the intensity of the radial flux. It is natural to suppose that these effects are due to 90° elastic scattering in plasma of a small fraction of particles in the radial flux.

The energy distributions of ions emitted in the longitudinal direction from the region near the end of the shock coil have a different form. Figure 7 shows the $(dn_i/d\mathscr{E}_{\parallel})_1$ curves obtained for the first peak on the oscillograms. When these curves are plotted on a semi-logarithmic scale, the result is a set of straight lines with different slopes corresponding to different values of n_0. It is clear that the fraction of high-energy ions increases with decreasing n_0.
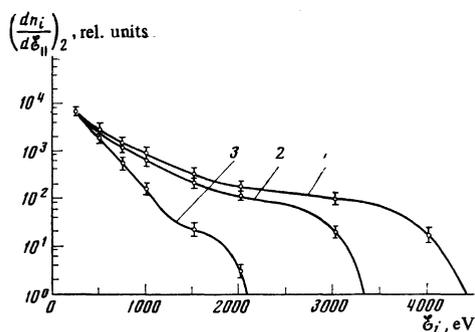
FIG. 6. Energy distribution of ions (normalized to $\mathscr{E}=260$ eV), $H_0=-600$ Oe; curve (1) $n_0 \approx 2 \times 10^{12}$ cm^{-3}; curve (2) $n_0 \approx 5 \times 10^{12}$ cm^{-3}; curve (3) $n_0 \approx 10^{13}$ cm^{-3}.
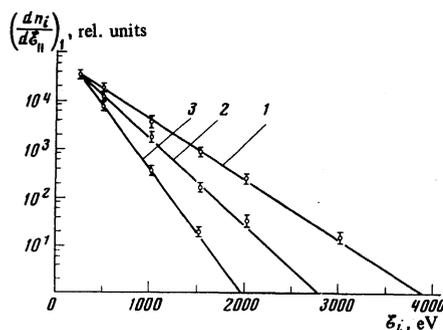
The observed difference between the spectra $(dn_i/d\mathscr{E}_{\parallel})_1$ and $(dn_i/d\mathscr{E}_{\parallel})_2$ may be an indication that the high-energy ions produced in the perturbed plasma in the two regions of space are due to different production mechanisms. The experimental data reported by Altyntsev et al.,[4] which indicate the presence of strong heating of the electron component of plasma in the neutral sheet, can be used as a basis for suggesting that the rapid escape of a fraction of hot electrons along the magnetic field produces a surplus of positive charges in the region of heating defined by the dimensions of the shock coil. This should lead to a potential discontinuity across the boundary separating the hot and cold plasmas. The existence of this discontinuity is confirmed by the data reported by Zolotovskiĭ et al.,[16] who used the configuration of a θ-pinch with opposing fields to investigate the excitation and properties of the thermal wave propagating along the magnetic field from the edge of the coil. The ions accelerated by this potential should produce a beam that diverges along the magnetic field on either side of the edges of the shock coil. The experiment records the fraction of this flux that escapes in the direction of the analyzer from the edge of the shock coil nearest to it.

The above model for the acceleration of ions in the edge region was verified by additional measurements in which the spectrum was examined in parallel magnetic fields ($H_1 \uparrow\uparrow H_0$). For the same parameters n_0 and H_0, it is known[4] that, under these conditions, one observes relatively weak heating of electrons, so that the potential accelerating the ions, whose magnitude should depend on the electron temperature, should be lower. Measurements have, in fact, revealed a considerable reduction in the maximum energy of the recorded ions. It is also important to note that the above dependence of the width of the spectrum $(dn_i/d\mathscr{E}_{\parallel})_1$ on the plasma concentration (Fig. 7) is in qualitative agreement with this model because $nT_e \propto (\Delta H)^2$ in the current sheet, and the electron temperature should decrease as n increases at constant ΔH.

Measurements of longitudinal spectra can thus be used to augment previously established experimental facts characterizing the process under investigation. We have shown that there are two regions, one in the central part of the shock coil and the other at its edge, from

which ions are emitted. The spectra of particles accelerated in the central region in the longitudinal and radial directions, $(dn_i/d\mathscr{E}_{\parallel})_2$ and $dn_i/d\mathscr{E}_{\perp}$, have identical properties. The intensity of the longitudinal flux is higher by roughly two orders of magnitude than that of of the radial flux. A broad spectrum of ions accelerated from the edge of the coil is observed.

DISCUSSION OF RESULTS

As already noted, the neutral sheet produced in the above experiments is collisionless and, therefore, collective processes play a decisive role in most of its characteristic properties. The presence of a turbulent region formed in the rarefaction or compression wave front ahead of the sheet is also an important factor that must be taken into account when the observed effects are interpreted.

Let us consider the reflection of ions from the neutral sheet. In contrast to the situation described by Dove,[5] the rotation of ions in the magnetic field of the piston under our conditions cannot lead to reflection because their cyclotron half-period, $t = 300$ nsec, exceeds the time at which the reflected beam is recorded ($t_1 = 120$ nsec). Consequently, the motion of the ions is affected mainly by the potential discontinuity due to the separation of the ion and electron charges in the sheet. It follows that, if we transform to the moving set of coordinates in which the neutral sheet is at rest, we can consider a thermally spread beam of plasma incident on a potential barrier of height φ_m. If we use this scheme, we can obtain a quantitative estimate for the fraction n_1/n_2 of reflected particles by using the reflection condition $\frac{1}{2}Mv_i^2 \le e\varphi_m$ (v_i is the velocity of ions in the moving set of coordinates) and the ion velocity distribution in the incident beam. It is also important to take into account the fact that this distribution function may not be the same as in the original preliminary plasma.[1] The above scheme could be confirmed by comparing n_1/n_2 with the experimental value but, as already noted, the absence of data on the characteristics of the potential discontinuity in the sheet prevents our carrying out this comparison.

We must now compare the results on the longitudinal flux of ions from the central part of the shock cell. The fact that the spectra $(dn_i/d\mathscr{E}_{\parallel})_2$ and $dn_i/d\mathscr{E}_{\perp}$ are similar shows that this flux can be associated with the 90° scattering of a small fraction of particles belonging to the radial flux in the plasma. Estimates show that the Coulomb scattering of the ion beam cannot ensure the observed intensity because the mean free path of particles with energies in the above ranges, i.e., $\lambda_C = 1/n_0\sigma_C \approx 10^3$–$10^6$ cm (σ_C is the Coulomb scattering cross section at 90°), is much greater than the size of the scattering target (~10 cm). The observed effect can, however, be explained by the scattering of ions by the turbulent electric fields in the perturbed plasma in the neutral sheet and in the rarefaction or compression wave. It is interesting to note that comparison of the longitudinal and transverse spectra obtained for similar values of n_0 and H_0 can be used to determine the shape of the

energy dependence of the scattering cross section $\sigma_{eff}(\mathscr{E})$. This comparison shows that, very approximately, $\sigma_{eff}(\mathscr{E}) \propto \mathscr{E}^{-1}$ whereas, for Coulomb scattering, $\sigma_C(\mathscr{E}) \propto \mathscr{E}^{-2}$.

Finally, analysis of the measured longitudinal particle flux can be used to propose that the appearance of ions accelerated across the boundary between the cold and hot plasmas is connected with the presence of a potential discontinuity on the thermal wave front. All that needs to be said here is that this model of accleration may not fully reflect the entire physics of the phenomena leading to the observed effect. In particular, turbulent processes in the thermal wave front may provide a substantial contribution to acceleration.

Elucidation of the role of these processes will require a more complete set of experimental data on the characteristics of turbulent electric fields and the potential discontinuity in the thermal wave front, as well as data on the heating of the electron component of the plasma under the shock coil.

---

[1] This is confirmed by the spectra of reflected particles leaving the sheet ($T_{i1} > T_i^0$). The change in the thermal spread in the incident flux may be connected with the presence of a turbulent zone in the rarefaction or compression wave front preceding the neutral sheet.[17]

---

[1]N. Kawashima and N. Ohyabu, Report No. 464, Tokyo University, 1971.

[2]A. G. Frank, Tr. Fiz. Inst. Akad. Nauk SSSR **74**, 108 (1974).

[3]A. T. Altyntsev and V. I. Krasov, Zh. Tekh. Fiz. **44**, 2629 (1974) [Sov. Phys. Tech. Phys. **19**, 1639 (1975)].

[4]A. T. Altyntsev, V. I. Krasov, and V. M. Tomosov, Preprint 5-76, SibISMIR, 1976.

[5]W. F. Dove, Phys. Fluids **14**, 2359 (1971).

[6]Yu. A. Berezin, R. Kh. Kurtmullaev, and Yu. E. Nesterikhin, Fiz. Goreniya Vzryva **1**, 3 (1966).

[7]V. E. Golant, Sverkhvysokochastotnye metody issledovaniya plazmy (Ultrahighfrequency Methods of Studying Plasma), Nauka, M., 1968, p. 74.

[8]V. V. Afrosimov, I. P. Gladkovskii, Yu. S. Gordeev, I. F. Kalinkevich, and N. V. Fedorenko, Zh. Tekh. Fiz. **30**, 1456 (1960) [Sov. Phys. Tech. Phys. **5**, 1378 (1961)].

[9]N. A. Koshilev and O. G. Parfenov, Zh. Prikl. Mekh. Tekh. Fiz. No. 6, 40 (1974).

[10]N. I. Alinovskii, A. T. Altyntsev, and N. A. Koshilev, Zh. Prikl. Mekh. Tekh. Fiz. No. 3, 132 (1970).

[11]N. I. Alinovskii, Author's Abstract of Thesis for Candidate's Degree, Institute of Nuclear Physics, Siberian Division, Academy of Sciences of the USSR, Novosibirsk, 1972.

[12]A. T. Altyntsev, N. A. Koshilev, V. L. Masalov, N. A. Strokin, V. M. Tomozov, A. A. Shishko, and V. N. Krasov, in: Abstracts of Papers and Brief Communications at the All-Union Conf. on Plasma Astrophysics, Nauka, Irkutsk, 1976, p. 64.

[13]A. T. Altyntsev, N. A. Koshilev, V. I. Krasov, V. L. Masalov, O. G. Parfenov, and A. A. Shishko, Pis'ma Zh. Eksp. Teor. Fiz. **18**, 397 (1973) [JETP Lett. **18**, 233 (1973)].

[14]R. Kh. Kurtmullaev, Doctoral Thesis, Institute of Nuclear

Physics, Siberian Branch, Academy of Sciences of the USSR, Novosibirsk, 1969.
[15]A. V. Gurevich, R. A. Salimov, and N. S. Buchel'nikova, Teplofiz. Vys. Temp. **7**, 852 (1969).
[16]O. A. Zolotovskiĭ, V. I. Koroteev, R. Kh. Kurtmullaev, and

V. N. Semenov, Dokl. Akad. Nauk SSSR **197**, 564 (1970) [Sov. Phys. Dokl. **16**, 223 (1971)].
[17]G. E. Vekshteĭn and R. Z. Sagdeev, Pis'ma Zh. Eksp. Teor. Fiz. **11**, 297 (1970) [JETP Lett. **11**, 194 (1970)].
Translated by S. Chomet

Effective fields at diamagnetic impurities in rare-earth metals

P. V. Bogdanov, S. K. Godovikov, M. G. Kozin, V. V. Turovtsev, and V. S. Sh'pinel'

Nuclear Physics Research Institute of the Moscow State University
(Submitted April 2, 1976; resubmitted February 9, 1977)
Zh. Eksp. Teor. Fiz. **72**, 2120–2129 (June 1977)

The hyperfine fields at the nuclei of impurity ^{119}Sn atoms in metallic Tb were measured in the regions of ferromagnetic and antiferromagnetic ordering in the temperature range 4.2–235°K. A strong deviation (up to 90%) of the plot of the temperature dependence of the hyperfine field from the plot of the spontaneous magnetization of the matrix is observed. A comparison with analogous measurements for the Dy matrix shows that the exchange constants can depend on the helicoid angle α. To explain the temperature anomaly, we consider, besides the previously discussed mechanisms, also a new mechanism connection with the rotation of the moments of the nearest environment of the impurity atom.

PACS numbers: 75.30.Hx

The great variety of magnetic structures and the many magnetic properties of heavy rare-earth metals are attributed to the indirect exchange interaction of localized magnetic moments of the unfilled $4f$ shell via the conduction electrons and to interaction with the crystal field. According to the Ruderman-Kittel-Kasuya-Yosida (RKKY) model, the exchange interaction has an oscillating long-range character and leads to polarization of the conduction electrons. Information on the polarization of the conduction s electrons can be obtained from the magnetic field induced by them at the nuclei of a diamagnetic impurity. The investigation of the magnetic field at the nuclei of impurity tin in heavy rare-earth metals, carried out by the γ-resonance method, shows that the temperature dependence of these fields differs substantially from the magnetization curve for the matrix in the case of the Dy and Ho matrices.[1] An explanation of the observed anomalies within the framework of the s-f interaction model cannot be obtained without additional assumptions. A similar anomalous temperature dependence of the magnetic field at the impurity atom was confirmed in an investigation of the hyperfine interaction for another diamagnetic impurity (Cd) in the same matrices, carried out by the method of disturbed γ-γ correlations.[2,3]

In the present study we have used the γ-resonance method to perform more detailed measurements of the temperature dependence of the magnetic fields at Sn impurity nuclei in metallic Tb and Dy. The obtained data point to a complicated connection between the hyperfine field and the rotations of the moments on going from the collinear to the helicoidal type of order. We consider the possible mechanisms of the observed strong temperature anomalies of the hyperfine fields, and, in particular, the mechanism connected with the

fact that the matrix ions have an orbital angular momentum.

EXPERIMENTAL PROCEDURE

The preparation and investigation of polycrystalline Dy samples with 0.3–0.5 at.% Sn impurity, enriched to 86.9% Sn^{119}, is described in[4]. An analogous procedure was used also for Tb samples with 0.5 at.% Sn impurity, with additional measures taken to increase the accuracy of the temperature measurements, especially within the limits of the narrow antiferromagnetic region[5] (221–229 °K). To this end, a semiconducting resistance thermometer of the "KG" type was clamped with the aid of a beryllium spring to the center of the sample, where a chromel-gold thermocouple (0.4 at.% Fe) was also located and connected in an automatic-control circuit. In addition, to exclude the influence of parasitic thermal emf's, the readings of the pickup at opposite directions of the current were averaged. The temperature was maintained constant within $\leqslant 0.1$ °K, and the temperature gradient over the sample did not exceed 0.5 °K.

For investigations in a longitudinal magnetic field we used an installation with a superconducting solenoid that produced a field of intensity up to 40 kOe at a sample temperature of 4.2 °K.

RESULTS OF EXPERIMENTS

The characteristic form of the Mössbauer spectra in the case of Dy is shown in Fig. 1. The spectra have a complicated structure whose character changes qualitatively near the ferromagnetism–antiferromagnetism phase transition. The spectrum at 84 °K was obtained approximately a year after the others, and shows enhancement of the central part of the line spectrum, due